90% pump depletion and good beam quality in a pulse-injection-seeded nanosecond optical parametric oscillator

D. J. Armstrong and A. V. Smith

Lasers, Optics, and Remote Sensing Department, Sandia National Laboratories, Albuquerque, New Mexico 87185-1423

Received September 6, 2005; accepted September 26, 2005

We measured 90% pump depletion in a singly resonant image-rotating nanosecond optical parametric oscillator that was pulse-injection seeded by a self-generated signal pulse. The oscillator was pumped by an 8 ns duration single-frequency 532 nm pulse from an injection-seeded *Q*-switched Nd:YAG laser and resonated an 803 nm signal. The pump and pulsed-seed beams had flat-topped spatial fluence profiles with diameters of approximately 6 mm, giving a cavity Fresnel number at 803 nm approaching 400. The beam cleanup effects of the image-rotating cavity produce a far-field signal spatial fluence profile with approximately 60% of its energy falling within the diffraction-limited spot size.

OCIS codes: 190.4970, 190.4410, 140.4780.

When oscillation in a singly resonant nanosecond optical parametric oscillator (OPO) builds from quantum fluctuations in the signal and idler fields, buildup time τ_{BU} can be a substantial fraction of pump pulse duration τ_P. This is especially true near the oscillation threshold, where τ_{BU} is greatest, conversion efficiency η [=(signal energy+idler energy)/(pump energy)] is lowest, and pump power $P(t)$ remains largely undepleted for all $t < \tau_{BU}$.

As pump energy is increased above threshold, τ_{BU} decreases and η increases to $\gtrsim$50%, but eventually η diminishes due to parametric backconversion, where signal and idler light mix to generate new pump light. The reversal of energy flow and the accompanying π phase shift among these three waves not only reduces η but diminishes beam quality as well.[1]

Near threshold, a nanosecond OPO's efficiency can be improved by injection seeding with single-frequency cw light to reduce τ_{BU}. However, single-frequency operation does not eliminate backconversion, so at higher pump energy, η eventually equals the efficiency of unseeded oscillation. This means that the key to high η is achieving $\tau_{BU} \ll \tau_P$ with the pump energy slightly below the backconversion threshold. In principle, cw seeding can achieve $\tau_{BU} \ll \tau_P$, but the required multikilowatt power levels are impractical, leaving pulsed seeding on nanosecond time scales as the only sensible approach. Seed energies of $\gtrsim$1 mJ are usually sufficient, with the additional requirements that the temporal Fourier transform of the seed pulse overlap only one longitudinal mode of the OPO cavity and that the seed arrive earlier than the pump pulse by $\leqslant \tau_P$. A tunable pulsed laser or auxiliary single-frequency OPO can serve as an independent seed source, or, alternatively, the OPO can seed itself when an early-arriving pump pulse generates a seed pulse that is subsequently injected into the cavity. A self-generated seed is practical because its spectrum matches the OPO's cavity resonances, eliminating the need to frequency stabilize one pulsed oscillator relative to another. One implementation of this technique used a grating to spectrally filter the broadband seed pulse to achieve tunable single-mode oscillation.[2] Our method, depicted in Fig. 1, uses cw seeding and backward pumping in a nonplanar ring-cavity Ristra OPO[3] to generate a single-frequency seed pulse. We found that injected seed energies of $\geqslant$50 μJ reduce τ_{BU} to $\leqslant 0.1\tau_P$, and energies of $\geqslant$1 mJ result in $\tau_{BU} \ll \tau_P$, making possible pump depletion of 90%.

Pulsed seeding in almost any form increases η; however, in a singly resonant OPO, pump depletion of $\gtrsim$65% requires careful selection of all operating parameters. These include the cavity configuration and its effect on beam quality of the resonated wave, the crystal type and its phase-matching conditions, the crystal length, output coupling, and the spatial profiles of the pump and pulsed-seed beams (ideally flat-topped for optimum mixing efficiency). Before laboratory evaluation, all these parameters in our design were optimized by numerical modeling.[3,4]

From modeling and from measurements with a pulsed-seeded Ristra OPO, we determined that flat-topped spatial profiles are essential for obtaining pump depletion near 90%. We have also found that, if the pump profile is flat, the spatial profile of the pulse-seed beam largely determines the profile of the OPO's resonated wave. Consequently, use of flat-topped spatial profiles is essential in our experiment. To obtain a flat profile for the pulsed seed we converted the near-Gaussian low-energy small-diameter backward signal pulse into a large-diameter flat-topped beam by using spatial filtering and a Gaussian-to-flat-top refractive beam shaper. A similar beam-shaping technique was applied to our forward pump laser, such that its spatial profile and diameter closely matched those of the pulsed seed beam.[5]

Figure 2 shows the results of averaging 503 pulses; the average depletion and rms variation in depletion are 88.2% and 0.53%, respectively, with a maximum single-shot depletion of 89.8%. The normalized signal and pump pulses possess nearly identical temporal

0146-9592/06/030380-3/$15.00

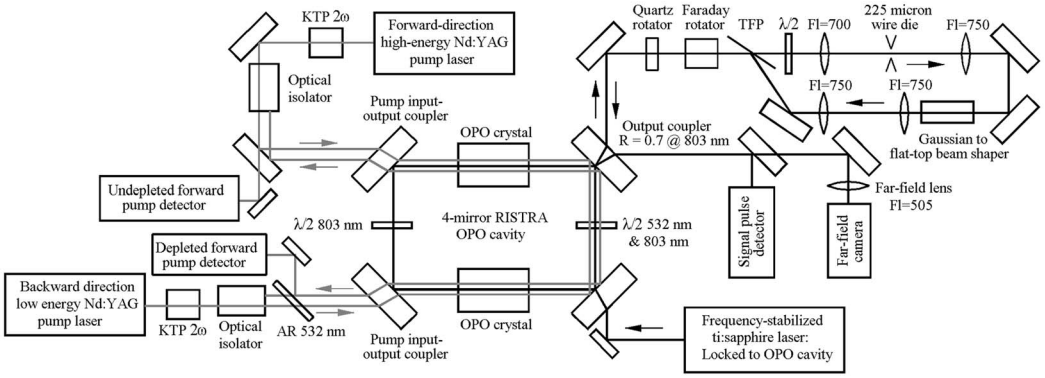

Fig. 1. Block diagram of the experiment. The nonplanar Ristra OPO cavity,[3] denoting a rotated image singly resonant twisted rectangle, is projected onto the plane of the page. The 109 mm long cavity contains two 10 mm × 10 mm × 15 mm KTP crystals cut at $\theta = 58°$, $\phi = 0°$ for $803(e) + 1576.4(o) \rightarrow 532(o)$. Intracavity $\lambda/2$ retardation maintains pump and signal polarizations parallel to the crystal eigenpolarizations. Approximately 5 mW of 803 nm light from a frequency-stabilized cw Ti:sapphire laser (Coherent 899) is dither locked to a cavity fringe by use of phase-sensitive detection, so the laser providing a small-diameter low-energy backward-direction pump beam (Q-switched injection-seeded Nd:YAG, Continuum NY82-10) generates a 2 mm $1/e^2$ diameter single-frequency 5 mJ seed pulse. The seed pulse returns to the cavity via the optical path containing a spatial filter, a Gaussian-to-flat-topped refractive beam shaper (Newport GBS-AR16), and an imaging telescope, with maximum energy measured at a thin-film polarizer (TFP) of >1.5 mJ. The 6 mm diameter spatially flat pulsed seed resonates in the cavity and is amplified by the time-delayed forward pump laser (Q-switched injection-seeded Nd:YAG, Continuum PL-9010). The pump laser was modified to have a high-quality flat-topped profile closely matching that of the pulsed-seed beam.[5] Relative arrival times of the pulses are controlled to ~1 ns by external triggering of the pump lasers with clock-synced digital delay generators (SRS DG535). Signal and forward pump detectors are Hamamatsu R1328U vacuum photodiodes. R, reflection; AR, antireflecting; Fls, focal lengths.

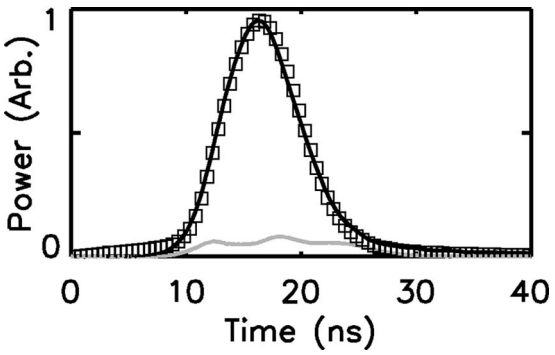

Fig. 2. Temporal profiles for the undepleted pump (solid darker curve), depleted pump (solid lighter curve), and OPO signal (open squares); the pump depletion calculated from the average of 503 pulses was 88%, with maximum single-shot depletion of 90%. The peak height of the undepleted pump and signal are normalized, with the depleted pump on the same scale as the undepleted pump. The unseeded signal (not shown) was intermittent during data acquisition and barely observable after averaging, because the pump energy was near or below the threshold for unseeded oscillation.

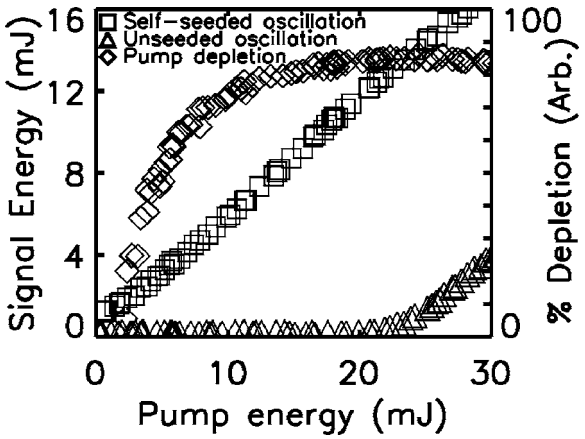

Fig. 3. Energy efficiency curves for pulse-seeded and unseeded oscillation, and for pump depletion with pulsed seeding, plotted versus forward pump energy. See text for details.

profiles because $\tau_{BU} \approx 0$ and $\eta_{average} > 88\%$. Care must be taken to accurately measure pump depletion at these levels. Referring to Fig. 1, we begin by blocking the cw seed laser, backward pump laser, and OPO cavity such that there is no oscillation or single-pass amplification within the cavity. We then digitize pulses returned by the depleted and undepleted forward-pump detectors, using a Tektronix TDS 7154B digital phosphor oscilloscope. Subsequent temporal integration and averaging of 100 or more pulses provides a ratio of these two pulse areas. When oscillation resumes, knowledge of this ratio allows real-time monitoring of shot-to-shot pump depletion. Postacquisition processing determines average and rms depletion.

To compare pulse-seeded to unseeded efficiency, we recorded signal energy and pump depletion versus pump energy, with the results shown in Fig. 3. We used two 15 mm long OPO crystals to achieve high depletion for low pump fluence, and Fig. 3 shows ~85% depletion with ~14 mJ of signal energy when the pump energy is 25 mJ (fluence, 0.09 J/cm^2), which is slightly above the unseeded oscillation threshold. We note that 85% depletion is easily reproduced by our apparatus, whereas 90% single-shot depletion for the data in Fig. 2 requires achieving interferometric alignment of the pulsed-seed beam simultaneously with $\Delta k = 0$ in both crystals: a delicate, iterative process. Note that the curve for pulse-

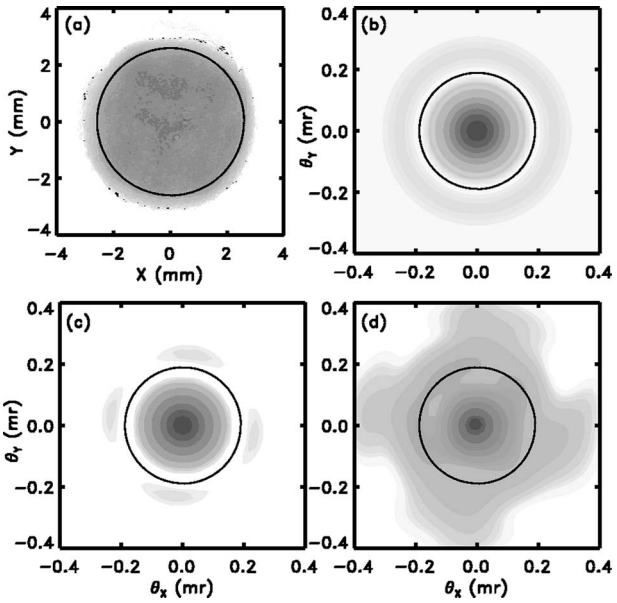

Fig. 4. Signal spatial fluence profiles. (a) Measured near field; the circle denotes a flat-topped diameter of 5.2 mm. (b) Reference Airy pattern generated by Fourier transforming a true flat top of 5.2 mm diameter with the circle at the first Airy null enclosing 84% of energy. (c) Far-field fluence obtained by Fourier transforming the near-field fluence in (a). (d) Measured far-field fluence with approximately 60% of the energy within the circle. θ_x, θ_y, far-field angles. See text for additional details.

seeded oscillation suggests that threshold occurs for <0 mJ pump energy, but this anomaly is due to the energy of the seed pulse. Although these measurements show only near-threshold efficiency, at higher pump energy backconversion eventually leads to nearly equal seeded and unseeded efficiency. However, the nearly identical signal and undepleted pump temporal profiles occur only for pulsed seeding. This temporal matching enhances the efficiency of subsequent mixing processes such as sum-frequency generation, in which an undepleted pump mixes with the OPO's signal to generate UV radiation.

The uniform fluence of flat-topped spatial profiles optimizes OPO efficiency and, for large diameters, fluence remains low for high-energy operation, reducing the risk of optical damage. We selected 6 mm diameter flat-topped beams for these reasons, but this choice results in a cavity Fresnel number ($\mathcal{F}=D^2/\lambda L$, where D denotes diameter and L is the round-trip cavity length) approaching 400 at $\lambda=803$ nm. For non-image-rotating cavities, $\mathcal{F}>100$ generally results in poor beam quality but, as explained in Ref. 3, image rotation working in conjunction with angle-critical birefringent phase matching can produce highly symmetric high-quality beams, even for large $\mathcal{F}$.

Figure 4(a) shows the measured near-field signal spatial fluence, with the 5.2 mm diameter circle denoting the flat-topped portion of the beam. Absent phase distortions, propagation to the far field forms an Airy pattern, as shown by the reference far-field fluence in Fig. 4(b), which we obtained by Fourier transforming a true 5.2 mm diameter flat-topped profile. Figure 4(c) shows the far-field fluence obtained by transforming the entire near-field profile in Fig. 4(a), assuming no phase distortion, with the circles in Figs. 4(b) and 4(c) denoting the first Airy null. Figure 4(d) shows the experimental far-field signal fluence measured through a 505 mm focal-length lens with an effective f-number of $\sim$80. The structure in Fig. 4(d) could arise from phase front distortion but might also reflect the temporal dynamics of a real OPO signal pulse, which are neglected by the time-independent transform of Fig. 4(c). Nonetheless, spatial integration of the measured fluence in Fig. 4(d) reveals that approximately 60% of the energy falls within the first Airy null, a good result for a cavity with $\mathcal{F}\approx400$. We also note the excellent pointing stability of the signal beam. From 200 measurements of the far-field centroid position the rms variation of the vertical and horizontal tilts is $\leqslant2.5$ μrad, or $<1\%$ of the diffraction limit. Fluctuations in beam pointing of this size can probably be attributed to refractive turbulence from air movement in the laboratory.

Finally, although self-generated pulsed seeding resulted in 90% pump depletion ($\eta\approx90\%$), the optical efficiency for the entire system is lower because the backward pump energy was as high as 20 mJ. A flat-topped backward-pump profile, rather than the Gaussian profile used in the experiment, could improve efficiency. Other methods, such as pulsed idler seeding, might raise net system efficiency as well.

The authors acknowledge financial support from NASA Langley Research Center, Hampton, Va. Sandia is a multiprogram laboratory operated by Sandia Corporation, a Lockheed Martin Company, for the U.S. Department of Energy's National Nuclear Security Administration under contract DE-AC04-94AL8500. D. J. Armstrong's e-mail address is darmstr@sandia.gov.

References

1. G. Anstett, M. Nittman, and R. Wallenstein, Appl. Phys. B **79**, 305 (2004).
2. Y. He and B. J. Orr, in *Conference on Lasers and Electro-Optics*, Vol. 88 of OSA Trends in Optics and Photonics Series (Optical Society of America, 2003), pp. 2–6.
3. A. V. Smith and D. J. Armstrong, J. Opt. Soc. Am. B **19**, 1801 (2002).
4. A. V. Smith, W. J. Alford, T. D. Raymond, and M. S. Bowers, J. Opt. Soc. Am. B **12**, 2253 (1995).
5. D. J. Armstrong and A. V. Smith, in Proc. SPIE **5525**, 88 (2004).